

Glitch rises as a test for rapid superfluid coupling

arXiv: 1804.02706

in collaboration with A. Cumming & N. Andersson

COSPAR, E1.10

July 17, 2018

Vanessa Graber, McGill University

vanessa.graber@mcgill.ca



- **Glitches** are sudden spin-ups caused by angular momentum transfer from a crustal superfluid, decoupled from the lattice (and everything tightly coupled) due to vortex pinning (Anderson and Itoh, 1975).
- Catastrophic vortex unpinning triggers the glitch and frictional forces acting on the **free vortices** govern the **neutron star's post-glitch response**. Observations suggest that **crust spin-up** after a glitch is very fast (Dodson et al., 2007; Palfreyman et al., 2018).
- Within **hydrodynamical models**, this recoupling is captured via a dimensionless **mutual friction** coefficient \mathcal{B} . It is directly connected to the **mesoscopic dynamics**, because a single vortex experiences a resistive force $f_{\text{res}} = \rho_s \kappa \mathcal{R} \Delta v$ and $\mathcal{B} = \mathcal{R}/(1 + \mathcal{R}^2)$.

Learn about the small-scale physics by analysing the glitch rise.

- Different processes affect **vortex dynamics** in the crust and the core:
 - ▶ phonon excitations (Jones, 1990)
 - ▶ Kelvin wave excitations (Epstein and Baym, 1992; Jones, 1992)
 - ▶ electron quasi-particle scattering (Feibelman, 1971)
 - ▶ scattering of electrons off the vortex magnetic field (Alpar et al., 1984; Andersson et al., 2006)
 - ▶ Kelvin wave excitations (Link, 2003)
- Focus on **Kelvin wave excitations** in the crust, dominating the initial recoupling (if vortex-nucleus velocity is $\Delta v \gtrsim 10^2 \text{ cm s}^{-1}$ (Jones, 1992)).
- We reanalyse the works of Epstein and Baym (1992) and Jones (1992), using a **simple argument** to understand discrepancies between both formalisms and **calculate the drag** \mathcal{R} for realistic crust parameters.



- In the absence of forces, a vortex supports **Kelvin waves** with angular frequency $\omega_k = Tk^2/\rho_s\kappa = \hbar k^2/2\mu(k)$ (Thomson, 1880), with tension T and effective mass $\mu(k) \simeq -2m_u/\ln k\xi$.
- Vortex-nucleus **interactions** excite waves with wave numbers $k \lesssim k_* \equiv (2\mu\Delta v/\hbar l)^{1/2} \Rightarrow$ determine the power p transferred into Kelvin waves and relate it to the **resistive force**, $f_{\text{res}} = p/\Delta v$.
- Epstein & Baym and Jones make **different assumptions** about p and the interaction potential including the typical interaction scale l :

$$E_{\text{EB}}(s) = \frac{E_s}{(1 + s^2/R_N^2)^4} + \frac{E_l}{1 + s^2/R_N^2}, \quad E_J(s) = E_p \exp\left(-\frac{s^2}{2\xi^2}\right), \quad (1)$$

where s is the separation, E_s (E_l) a short-range (long-range) interaction contribution, R_N the nuclear radius and ξ the coherence length.

- Drag coefficients depend on the relative **vortex-nucleus velocity**, but E_p and Δv are connected by a mesoscopic force balance, $\Delta v \simeq f_{\text{pin}}/\rho_s \kappa \sim E_p/la\rho_s \kappa$, for a pinning force f_{pin} per unit length and lattice spacing a .
- Correcting several errors in Epstein and Baym (1992) and accounting for a **reduction factor** δ due to averaging the microscopic pinning interaction over a mesoscopic vortex length scale (Seveso et al., 2016), we find

$$\mathcal{R}_{\text{EB}} \simeq 2.8 \left(\frac{\mu}{\hbar}\right)^{1/2} \left(\frac{E_p \delta}{\rho_s \kappa}\right)^{1/2} \frac{R_N}{a^{3/2}},$$

$$\mathcal{R}_J \simeq \frac{1}{2\sqrt{\pi}} \left(\frac{\mu}{\hbar}\right)^{1/2} \left(\frac{E_p \delta}{\rho_s \kappa}\right)^{1/2} \frac{a^{1/2}}{\xi}, \quad (2)$$

with $E_p^2 \simeq E_s^2 + E_1 E_s + 0.5 E_1^2$ in Epstein and Baym's formalism.

Calculate $\mathcal{B} \simeq \mathcal{R}$ for a realistic crust model based on three different microscopic models.

- We use the **crustal composition** of Negele and Vautherin (1973) and pinning **interaction parameters** from Epstein and Baym (1992) and Donati and Pizzochero (2006) to calculate \mathcal{R} in the inner crust.
- The **bottom of the crust** carries the majority of the crustal mass.

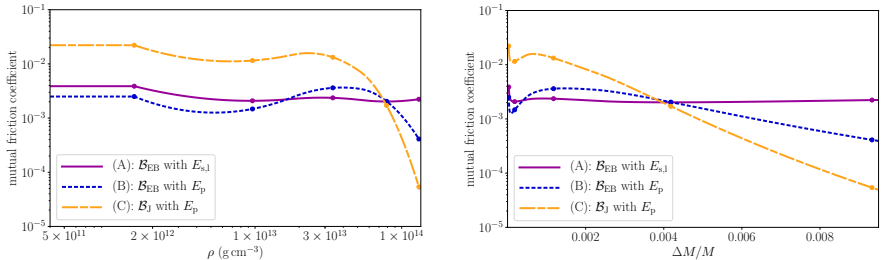


Figure 1: Mutual friction strength for kelvin wave coupling as a function of (left) density and (right) relative overlying mass fraction.

- Decompose the neutron star into crust superfluid, core superfluid and a non-superfluid 'crust' component. The latter two rotate rigidly and are coupled via a constant mutual friction coefficient $\mathcal{B}_{\text{core}}$.
- Neglecting entrainment for simplicity, the **equations of motion** are

$$\dot{\Omega}_{\text{sf}} = \mathcal{B} \left[2\Omega_{\text{sf}} + \tilde{r} \frac{\partial \Omega_{\text{sf}}}{\partial \tilde{r}} \right] (\Omega_{\text{crust}} - \Omega_{\text{sf}}), \quad (3)$$

$$\dot{\Omega}_{\text{core}} = 2\mathcal{B}_{\text{core}}\Omega_{\text{core}} (\Omega_{\text{crust}} - \Omega_{\text{core}}), \quad (4)$$

$$\dot{\Omega}_{\text{crust}} = -\frac{N_{\text{ext}}}{I_{\text{crust}}} - \frac{I_{\text{core}}}{I_{\text{crust}}} \dot{\Omega}_{\text{core}} - \frac{1}{I_{\text{crust}}} \int \rho \tilde{r}^2 \dot{\Omega}_{\text{sf}} dV. \quad (5)$$

- Relate ρ and \tilde{r} in the crust by solving the **TOV equations** for a realistic EoS to obtain $\mathcal{B}(\tilde{r})$ and integrate (3)-(5) in cylindrical geometry for **Vela pulsar** ($\Omega_{\text{crust}}(0) \approx 70 \text{ Hz}$, $\Delta\Omega_{\text{crit}} \approx 10^{-2} \text{ Hz}$).

- Solve equations for two **fiducial crust-core couplings**: $\mathcal{B}_{\text{core}} \sim 5 \times 10^{-5}$ (electron-vortex scattering) and $\mathcal{B}_{\text{core}} \sim 10^{-2}$ (Kelvin wave excitations).
- The superfluid rotates **differentially** due to the $\mathcal{B}(\tilde{r})$ -dependence. In the outer layers, \mathcal{B} is strongest and the superfluid couples within ~ 100 ms. Eventually, the superfluid has transferred all excess angular momentum and spun down to a **new steady state**, where all components corotate.

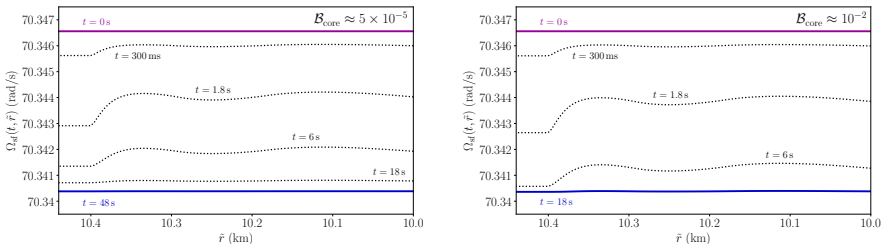


Figure 2: Ω_{sf} as function of radius and time calculated for drag profile (A) and two crust-core couplings.

- We compare different **friction profiles** by computing the change in crust frequency $\Delta\nu$. The glitch rise shape depends crucially on the **relative strength** of the crust and core mutual friction.
- For $\mathcal{B}_{\text{core}} \sim 5 \times 10^{-5}$: crustal coupling is faster than core coupling, creating a characteristic **overshoot** feature. The onset of crust-core coupling is visible as a break in the **phase shift** ϕ .

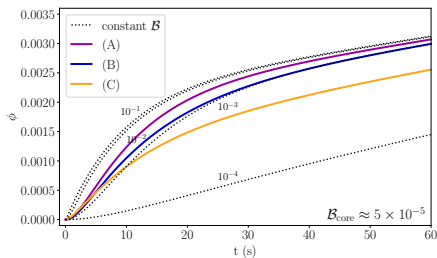
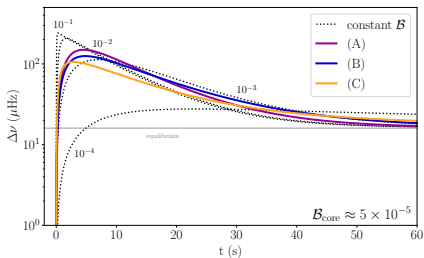


Figure 3: Change in crustal frequency $\Delta\nu(t) = [\Omega_{\text{crust}}(t) - \Omega_{\text{crust}}(0)]/2\pi$ and phase shift $\phi = \int \Delta\nu dt$ with time.

- For $\mathcal{B}_{\text{core}} \sim 10^{-2}$: crustal coupling is slower than core coupling, causing the glitch rise to be **monotonic in time**. The onset of crust-core coupling is not visible in the **phase shift** ϕ .

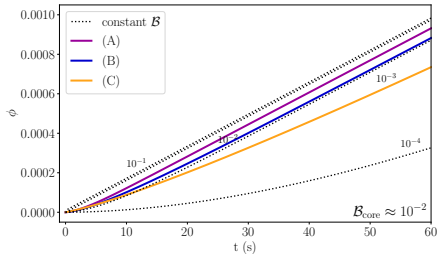
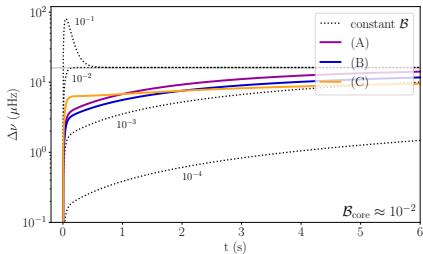


Figure 4: Change in crustal frequency $\Delta\nu(t) = [\Omega_{\text{crust}}(t) - \Omega_{\text{crust}}(0)]/2\pi$ and phase shift $\phi = \int \Delta\nu dt$ with time.

Detecting a break in phase shift allows us to constrain $\mathcal{B}_{\text{core}}$.

- First single-pulse observations of a glitch in the Vela pulsar (Palfreyman et al., 2018) allow a **comparison** between the data and our predictions.
- Model **timing residuals** $\Delta t \simeq -2\pi\phi/\Omega_{\text{crust}}(0)$ are compared to observed residuals. We include a shift $\Delta t_0 \approx 0.22$ ms at the time of the glitch.

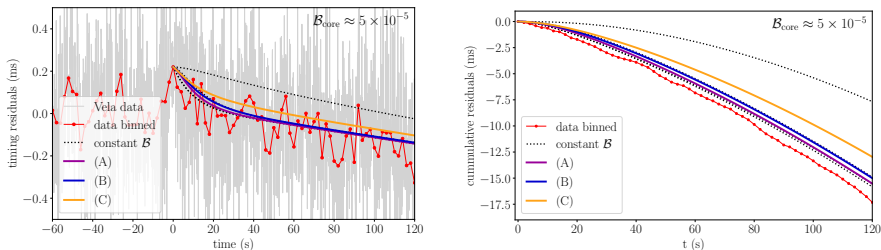


Figure 5: Comparison between theoretical (left) timing residuals and (right) cumulative residuals for $B_{\text{core}} \approx 5 \times 10^{-5}$ and observations of the 2016 Vela glitch.

Shape is rather insensitive to crustal profiles as long as $B \gtrsim 10^{-3}$.

- Analyse how sensitive the glitch rise is to $\mathcal{B}_{\text{core}}$ for crustal profile (A):

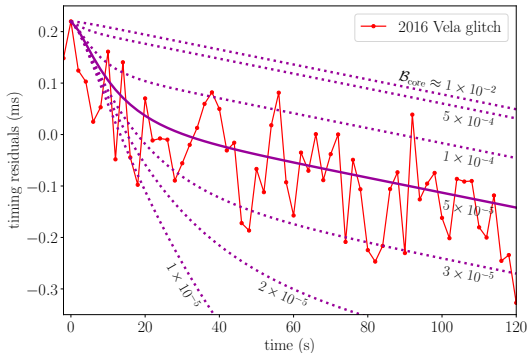


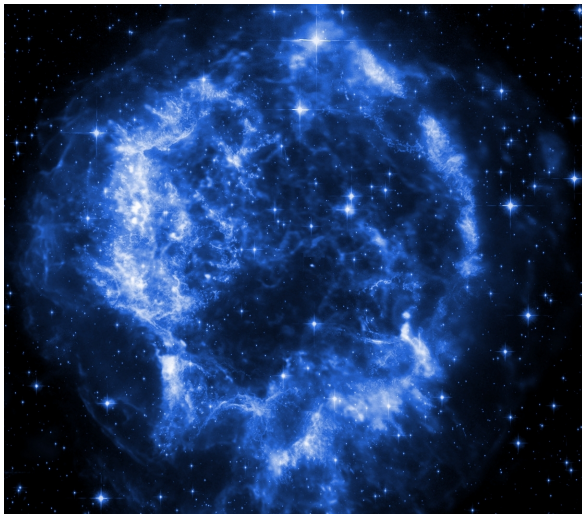
Figure 6: Comparison between the 2016 Vela glitch data and theoretical predictions calculated for drag profile (A) and a varying crust-core mutual friction strength $\mathcal{B}_{\text{core}}$.

The data would suggest a narrow range $3 \times 10^{-5} \lesssim \mathcal{B}_{\text{core}} \lesssim 10^{-4}$.

Conclusions

- In order to **constrain microphysics** of neutron stars, we need to understand the connection between the macroscopic observables and microphysics \Rightarrow **develop a predictive glitch rise model**.
- Combine realistic **Kelvin-wave profiles** in the crust with a simple treatment of the core mutual friction and implement both in a **three-component** neutron star framework \Rightarrow **glitch shape depends crucially on the relative strength between \mathcal{B} and $\mathcal{B}_{\text{core}}$** .
- **Comparison** between our models and the first pulse-to-pulse **glitch observations** suggest strong crustal combined with weak core mutual frictional \Rightarrow **i.e. $\mathcal{B} \gtrsim 10^{-3}$ and $3 \times 10^{-5} \lesssim \mathcal{B}_{\text{core}} \lesssim 10^{-4}$** .

The end



- Alpar, M. A., Langer, S. A., and Sauls, J. A. (1984). Rapid postglitch spin-up of the superfluid core in pulsars. *ApJ*, 282:533–541.
- Anderson, P. W. and Itoh, N. (1975). Pulsar glitches and restlessness as a hard superfluidity phenomenon. *Natur*, 256(5512):25–27.
- Andersson, N., Sidery, T., and Comer, G. L. (2006). Mutual friction in superfluid neutron stars. *MNRAS*, 368(1):162–170.
- Chamel, N. (2008). Two-fluid models of superfluid neutron star cores. *MNRAS*, 388(2):737–752.
- Dodson, R., Lewis, D., and McCulloch, P. (2007). Two decades of pulsar timing of Vela. *Ap&SS*, 308(1-4):585–589.
- Donati, P. and Pizzochero, P. M. (2006). Realistic energies for vortex pinning in intermediate-density neutron star matter. *PhLB*, 640(3):74–81.
- Epstein, R. I. and Baym, G. (1992). Vortex drag and the spin-up time scale for pulsar glitches. *ApJ*, 387:276–287.
- Feibelman, P. J. (1971). Relaxation of Electron Velocity in a Rotating Neutron Superfluid: Application to the Relaxation of a Pulsar's Slowdown Rate. *PhRvD*, 4(6):1589–1597.
- Ho, W. C. G., Glampedakis, K., and Andersson, N. (2012). Magnetars: super(ficially) hot and super(fluid) cool. *MNRAS*, 422(3):2632–2641.
- Jones, P. B. (1990). Rotation of the neutron-drip superfluid in pulsars: The resistive force. *MNRAS*, 243:257–262.
- Jones, P. B. (1992). Rotation of the neutron-drip superfluid in pulsars: The Kelvin phonon contribution to dissipation. *MNRAS*, 257(3):501–506.
- Link, B. (2003). Constraining Hadronic Superfluidity with Neutron Star Precession. *PhRvL*, 91(10):101101.

- Negele, J. W. and Vautherin, D. (1973). Neutron star matter at sub-nuclear densities. *NuPhA*, 207(2):298–320.
- Palfreyman, J., Dickey, J. M., Hotan, A., Ellingsen, S., and van Straten, W. (2018). Alteration of the magnetosphere of the Vela pulsar during a glitch. *Natur*, 556(7700):219–222.
- Seveso, S., Pizzochero, P. M., Grill, F., and Haskell, B. (2016). Mesoscopic pinning forces in neutron star crusts. *MNRAS*, 455(4):3952–3967.
- Steiner, A. W., Prakash, M., Lattimer, J. M., and Ellis, P. J. (2005). Isospin asymmetry in nuclei and neutron stars. *PhR*, 411(6):325–375.
- Thomson, W. (1880). Vibrations of a columnar vortex. *PMag*, 10(61):155–168.